Multiplex transport and detection of cytokines using kinesin-driven molecular shuttles

Lynnette Rios and George D. Bachand*

Received 19th September 2008, Accepted 28th November 2008
First published as an Advance Article on the web 5th January 2009
DOI: 10.1039/b816444d

The application of biomolecular active transport systems offers a potential route for downscaling multiple analyte assays for lab-on-a-chip applications. Recently, the capture and transport of a wide range of target analytes including proteins, virus particles, and DNA have been demonstrated using kinesin-driven molecular shuttles. The molecular shuttles consisted of microtubule (MT) filaments that were functionalized with either analyte-selective antibodies or complementary DNA, thus facilitating selective target capture and transport. In the present work, we have applied this microfluidic platform for the simultaneous detection of multiple target protein analytes. Multiplexing of molecular shuttles was achieved by immobilizing biotinylated antibodies against interleukin-2 (IL-2) and tumor necrosis factor-α (TNF-α) on biotinylated MTs using a streptavidin bridge. Nanocrystal quantum dots of different sizes and spectral emissions were functionalized with IL-2 and TNF-α antibodies to facilitate multiplexed detection. In this paper we discuss the results of selectivity and motility in single and multiplexed assays.

Introduction

Immunoassays are valuable tools for diagnostic and other analytical sciences with many methods in the market and more being developed every year. While most methods have been developed for single analyte detection, new research is focused on methods for detecting multiple analytes in a given sample. The majority of existing multiple analyte assays consist of array-based biosensors.[1,2] These arrays are constructed by injecting the primary antibody in a waveguide by means of a rubber stamp and using a fluidic device to flow the sample and labelled-antibody perpendicular to the immobilized capture antibody.[1,3] Other systems use inkjet printers to construct antibody lines or dots on the surface of silanized glass to form arrays.[2] Sample analysis in multiple analyte systems, however, becomes problematic due to the dependence on the signal from a single label and the immobilization of only one type of antibody per analyte. Two systems have overcome these limitations by using multiple fluorophores to identify each of the analytes: Delfia and Luminex. While these systems have been implemented for specific applications,[4–7] miniaturization of these technologies at the nanoscale level in lab-on-a-chip (LOC) applications has not been reported. In many cases, miniaturization of multiplex systems is prohibited by intrinsic limitations of the array approach and the complex fluidic devices required for use (*e.g.*, the use of long tubing, pumps and an external electricity source for operation).

The use of a biomolecular motor protein-based transport system represents a tremendous opportunity to develop LOC nanodevices that do not require pumps, fluidic systems, or external energy input.[8–10] Inside cells, biomolecular motors such as kinesin and dynein carry cargo along microtubules (MTs), which are hollow, cylindrical filaments that are ~25 nm in diameter and tens of microns in length. MTs self-organize into three-dimensional networks along which kinesin motors transport macromolecular cargo to various regions through the cell.[11,12] Kinesin is a dimeric protein that walks processively along MTs in 8 nm steps through an asymmetric hand-over-hand mechanism.[13–16] This system has been replicated for *in vitro* nanotechnological applications by immobilizing kinesin motors on a solid surface, and introducing MTs (and attached cargo) and ATP (*i.e.*, motor fuel).[8,10,17–19]

A prototypic, bioanalytical sensor based on *in vitro* kinesin-driven transport may be conceptualized to consist of three functional modules (Fig. 1). In the first module, antibody-functionalized MTs selectively capture multiple analytes from an introduced sample. Next, the captured analytes are separated from non-target analytes, and shuttled into an area in which analyte-selective fluorescent tags are transferred to antigens upon contact. Finally, the captured and tagged analytes are transported to the detection module. Such a device would be widely applicable for LOC scenarios in which pressure-driven or electrokinetic pumping cannot be used (*e.g.*, remote sensing applications). Advantages of such devices also include its small size, low sample volume requirements, rapid analysis, and simple use (*i.e.*, little human intervention).

A number of crucial enabling technologies for developing biomolecular motor-powered devices have already been developed. The ability to capture, transport, and detect a wide range of target bioanalytes including proteins, virus particles, and nucleic acids has been demonstrated using kinesin-driven molecular shuttles.[8,10,18–24] In these examples, the MT shuttles were functionalized with antibodies that enable selective target capture and transport. Analyte capture and detection assays for nucleic acids have also been developed by conjugating DNA to

Biomolecular Interfaces & Systems Department, Sandia National Laboratories, PO Box 5800, MS 1303, Albuqeurque, NM, 87185-1303, USA. E-mail: gdbacha@sandia.gov; Tel: +1 (505) 844-5164

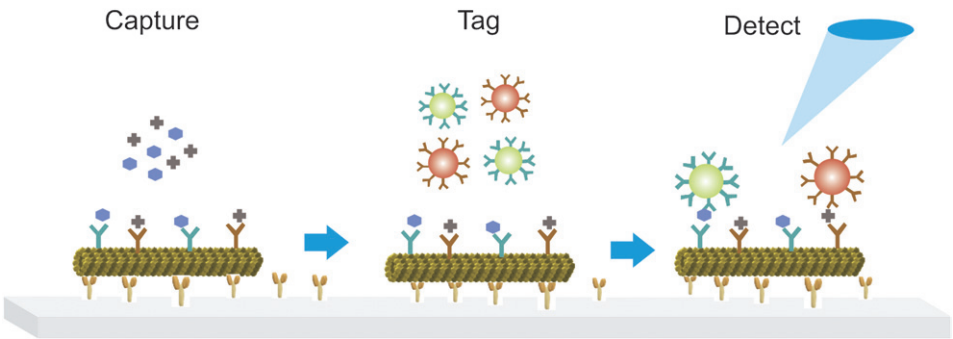

Fig. 1 Proposed device scheme for kinesin-driven multiple analyte assays. MTs functionalized with antibodies capture the analyte from a sample, and transport it along the kinesin-coated surface where the analyte is tagged with nQDs. Finally the MTs and tagged analyte reach the final module where nQDs are optically detected.

MT shuttles.[20,25] Recently, the ability to "pick-up" surface-tethered particles has been reported,[26] which represents a crucial mechanism for tagging captured analytes for subsequent detection in LOC systems. Controlling the direction of MT movement has been achieved using predefined channel geometries of the channels and surface chemistry.[27–30] MTs move in a straight path through junctions; therefore, junctions may be used for injecting antibodies, sample, buffer, and functionalized fluorescent tags. The ability to control motor transport[31–33] and preserve motor function and MT structure[34,35] in device architectures has been shown. A key near-term challenge in this area involves applying these technologies for multiple analyte assays, expanding the overall functionality of this system. To this end, we have developed and characterized a system that uses nanocrystal quantum dots (nQDs) to optically tag multiple analytes that have been captured by functionalized MT shuttles.

Method

Kinesin and MT preparation

Biotinylated MTs (bMTs) were formed by diluting biotinylated tubulin (Cytoskeleton) in BRB80 buffer (80 mM PIPES pH 6.9, 1 mM $MgCl_2$, 1mM EGTA) with 100 mM GTP and 5% glycerol, and polymerizing at 37 °C for 20–25 minutes. MTs were then stabilized by diluting 100-fold into BRB80T (BRB80 with 10 μM paclitaxel). MTs were further diluted in motility buffer (94 μL BRB80T plus 1 μL of each of the following: 2 M dextrose, 100 mM DTT, 20 mg mL^{-1} casein, 100 mM ATP, 0.8 mg mL^{-1} catalase, 2 mg mL^{-1} glucose oxidase). Motility buffer was also used to remove unbound material after incubation (wash steps). For all assays recombinant, a His-tagged kinesin motor originally isolated from *Drosophila melanogaster*[36,37] was expressed in *Escherichia coli* and purified using a Ni-NTA column as previously described.[23,38]

Nanocrystal quantum dot functionalization

To facilitate multiplexed detection, nanocrystal quantum dots (nQDs) of different sizes and spectral emissions (QDot® 605 and QDot® 525; Invitrogen Corp.) were functionalized with interleukin-2 (IL-2) and tumor necrosis factor-α (TNF-α) antibodies (nQD 525 with IL-2 antibody and nQD 605 with TNF-α antibody), and used to detect analytes bound to and transported on MTs. Initially, antibodies were conjugated to nQDs using biotin–streptavidin, but resulted in a high degree of non-specific binding, which was attributed to cross-reactivity of the streptavidin-coated nQDs with the biotinylated MTs; these results will be addressed in detail below. As an alternative approach, nQDs were directly functionalized with antibodies using the Antibody Conjugation Kit (Invitrogen Corp.), which covalently attaches antibodies to the nQDs. Briefly, nQDs were activated with the heterobifunctional crosslinker 4-(maleimidomethyl)-1-cyclo-hexanecarboxylic acid N-hydroxy-succinimide ester (SMCC). Following reduction with DTT to expose free sulfhydryls, antibodies were conjugated to the activated nQDs, and the reaction was quenched by β-mercaptoethanol. Antibody-functionalized nQDs were then purified by ultrafiltration using size exclusion chromatography.

Single and multiple analyte assays

Standard flow cells were constructed using a microscope slide, double-sided tape and a #1 glass coverslip.[37] A solution of casein (0.5 mg mL^{-1} in BRB80) was infused into a flow cell, followed by a solution of kinesin (~5 nM in BRB80 +0.2 mg mL^{-1} casein +1 mM MgATP) and incubated for 5 minutes. Selectivity was then engineered into the MT shuttles by attaching biotinylated antibodies selective for IL-2 and TNF-α on the bMTs using a streptavidin bridge. The bMTs were infused into the flow cell in motility solution (BRB80 + 0.2 mg mL^{-1} casein + 10 μM paclitaxel + 1 mM MgATP) and allowed to bind to kinesin for 10 minutes. A solution of 0.94 μM streptavidin was then added and allowed to react with the MTs for 10 minutes, followed by a 1 μg mL^{-1} mixture of primary antibodies and incubated for 10 minutes. To achieve multiplex detection, a solution containing both anti-TNF-α and anti-IL-2 antibodies was infused into the flow cell, resulting in the functionalization of MTs with both antibodies.

For the single analyte assay, a solution containing either TNF-α or IL-2 (1.0 μg mL^{-1}) in motility buffer was flowed through the cell followed by nQDs functionalized with secondary antibodies (nQD 525 with IL-2 antibody and nQD 605 with TNF-α antibody). Antibodies, proteins and functionalized nQDs were allowed to incubate for 10 minutes followed by wash steps using motility solution to remove excess material.

For the multiplex assay, a cocktail containing both TNF-α and IL-2 (1.0 μg mL^{-1}) was flowed through the cell. Following a wash step, nQDs previously functionalized with secondary antibodies (nQD 525 with IL-2 antibody and nQD 605 with TNF-α antibody) were infused into the flow cell. Antibodies, proteins and functionalized nQDs were allowed to incubate for 10 minutes followed by wash steps using motility solution to remove excess material.

All assays were analyzed using an Olympus IX71 microscope and 100× oil-immersion lens. Time-lapse and still frame images were collected using a CCD camera. MT velocity was calculated by subtracting sequential images and measuring the distance travelled over time using MicroSuite software. One-way Analysis of Variance (ANOVA) was used to evaluate significant difference among the velocities measured in the single and multiplexed assays.

Results and discussion

Assay selectivity was first tested by running single analyte assays. MTs were functionalized with IL-2 antibodies and tested against IL-2 antigen (positive control), as well as solutions containing no antigen (BRB80T buffer) or TNF-α in buffer as negative controls. These assays were then repeated with TNF-α in single analyte assays where the positive control contained only TNF-α, and the negative controls contained IL-2 or only buffer.

For single analyte assays, successful capture, tagging, and detection of the target analyte was achieved (Fig. 2). nQDs bound to MTs emitted green fluorescence when IL-2 analyte was present in the test cell, confirming the formation of a double antibody sandwich between the functionalized MTs and nQD 525 tags. Low or no binding of nQDs occurred when either a different antigen (TNF-α) or no antigen was infused into the test cell (Fig. 2A). Similar results were obtained for the TNF-α single analyte assay. nQDs bound to MTs emitted a red fluorescence signal only when TNF-α analyte was present in the sample (Fig. 2B). While a low level of non-specific binding was present in negative control samples, co-localization of nQDs on MTs was only observed in the presence of the TNF-α antigen. Overall these data indicate that the antibody combinations and functionalized nQDs are highly selective for the corresponding antigens. Such selectivity is crucial for analyzing mixed analyte samples.

Multiplexed detection of IL-2 and TNF-α was successfully achieved with MTs functionalized with two antibodies and the corresponding antibody-coated nQDS (Fig. 3). Both red and green nQDs were observed on MTs when both IL-2 and TNF-α antigens were present in a single sample. Yellow emission was also observed in these samples, suggesting that the red and green nQDs were within close proximity. Attachment of antibody-functionalized nQDs to MTs was not observed in negative control samples (*i.e.*, without analytes).

Selective capture and detection of the analytes was further optimized by reducing the level of background binding. A large factor in non-specific binding arose from the cross-reactivity of the nQDs and bMTs. Because bMTs were functionalized with biotinylated primary antibodies through a streptavidin bridge, binding of streptavidin-coated nQDs directly to the bMTs or primary antibodies resulted in non-selective attachment. Thus, the first approach to overcoming this non-specific interaction was to directly functionalize nQDs with the secondary antibody as described above. Eliminating the second streptavidin–biotin reaction greatly reduced non-selective background binding of nQDs in negative control assays (not shown).

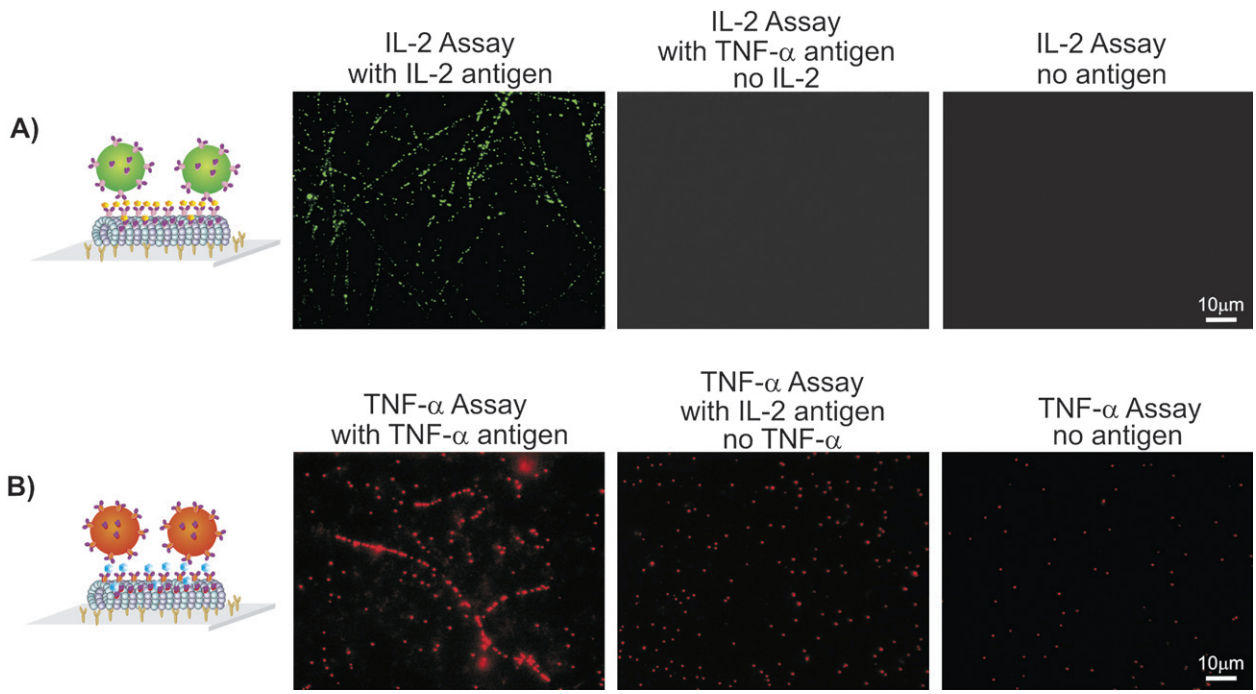

Fig. 2 Selectivity of single analyte assays. A: Selective detection in the IL-2 assay using green (525) nQDs for detection was observed only in the presence of antigen; no cross-reactivity with TNF-α was observed. B: Similarly, selective detection in the TNF-α assay using red (605) nQDs for detection was only observed when TNF-α was present; no cross-reactivity was observed with IL-2.

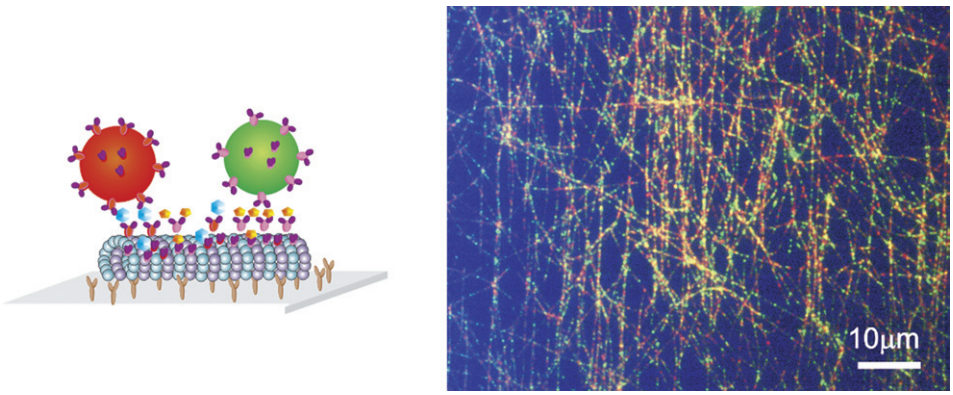

Fig. 3 Multiplex assay. The presence of green (Qdot® 525) and red (QDot® 605) nQDs on MTs confirmed capture of both IL-2 and TNF-α analytes in the multiplexed assays (artistic depiction, left). Red, green, and yellow fluorescence associated with individual MTs was observed (right). The yellow fluorescence suggested close spatial co-localization of the different nQDs (and analytes) on the MTs.

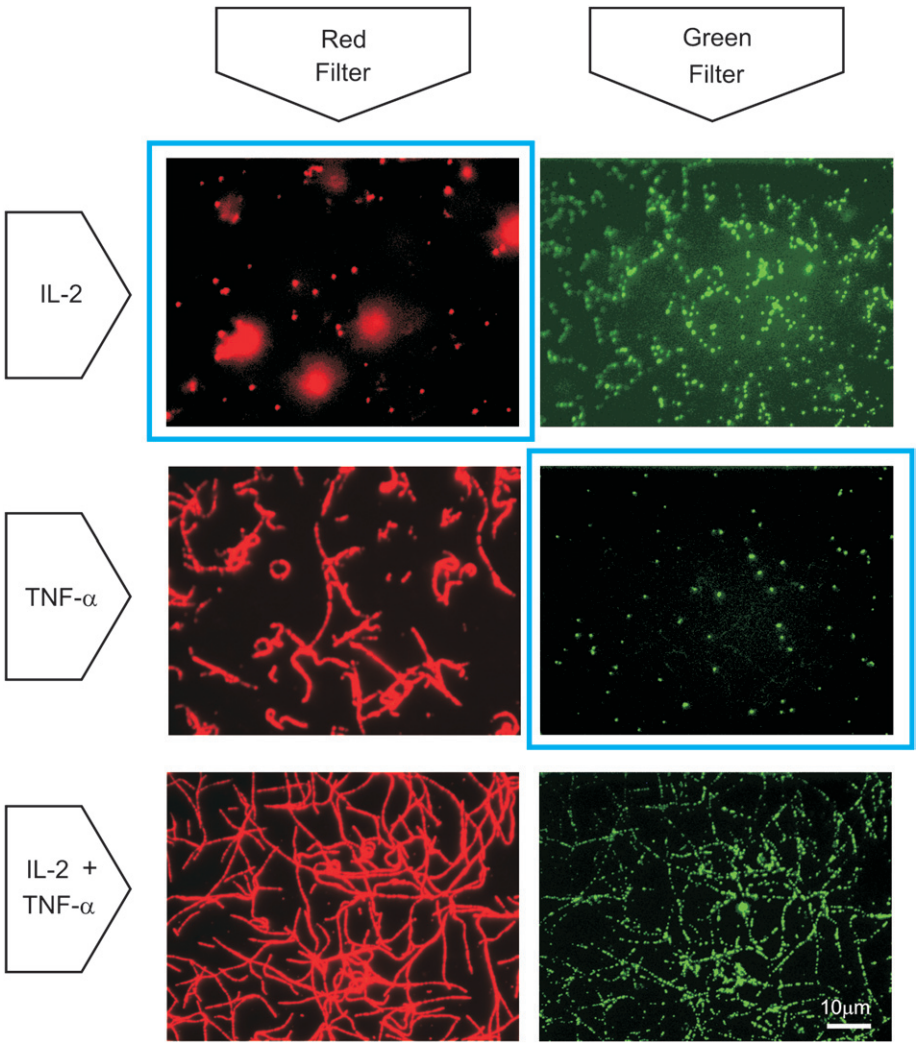

Fig. 4 Multiplex detection of IL-2 and TNF- α on molecular shuttles. Top row: Single analytes assay for IL-2 demonstrated selective binding of green nQDs to MTs only in the presence of IL-2 protein. Middle row: Selective detection of TNF-α was confirmed by the attachment of red nQDs only in the presence of the antigen. Bottom row: Both green and red nQDs bound to antibody-functionalized bMTs when both IL-2 and TNF-α were present in the multiplexed assay.

Table 1 Comparison of MT velocity (mean ± standard error) in single and multi-analyte detection assays

Motility assay type	Velocity MTs/μm s^{-1}
Biotin MTs	0.70 ± 0.01
Biotin MTs with streptavidin–nQDs	0.60 ± 0.02
IL-2 assay	0.37 ± 0.01
TNF-α assay	0.41 ± 0.01
Multiplex assay	0.37 ± 0.01

Increased selectivity was further achieved by optimizing methods such as blocking the surface of the flow cell with casein and washing excess protein after each incubation step. The effectiveness of casein concentration, as well as wash buffer (motility buffer) containing BSA (1% m/v) and Tween 20 (5% v/v) or motility buffer without BSA or Tween 20, was tested with respect to increased selectivity.

The lowest background nQD level was obtained by performing wash steps with motility buffer alone, without BSA or Tween 20 (Fig. 4). The IL-2 assay showed low non-selective binding in which red nQDs were dispersed and not associated with the bMTs. In fact, the majority of red nQDs were suspended in solution or bound directly to the surface, and may likely be removed with additional wash steps. The TNF-α assay also displayed low non-selective binding of green nQDs (Fig. 4). As expected the multiplex assay showed similar binding of both red and green nQDs, with very minimal non-specific binding.

A key aspect to developing LOC devices based on kinesin-powered molecular shuttles is maintaining motility of the complexes in order to achieve transport within a device. Thus, MT motility velocities were measured after capturing the double antibody sandwich assay (single and multi-analyte), and compared with unloaded MTs composed of 70% biotinylated tubulin, 20% unlabeled tubulin, 10% rhodamine-labeled tubulin as well as bMTs with streptavidin-coated nQDs attached (Table 1). A significant decrease in velocity was observed between bMTs and MTs transporting nQDs or bMTs in the single and multiplexed assays ($P < 0.001$). These results are consistent with results previously reported,[36] and directly related to increasing cargo density. The MT shuttles were, however, able to maintain transport velocities consistent with potential LOC applications.

Conclusions

We have demonstrated the simultaneous detection of multiple analytes in a sample using the kinesin-MT active transport system to capture and transport target analytes. The use of antibody-functionalized nQDs of different sizes enabled the detection of each analyte based on the distinct spectral emission. The application of kinesin-driven transport of antibody-functionalized MTs provides a platform for microfluidic systems that relies only on the conversion of chemical energy to mechanical work for the analysis of analytes in complex samples. Further, such motor protein-based systems eliminate the use of bulky pumping systems or large power requirement, which enables further miniaturization of devices for LOC applications. Detailed characterization of this technology will be needed to determine the lower limits of detection, and further optimization may be necessary to achieve detection in clinically relevant samples. Moreover, this multiplexed capture and transport system must be integrated with micro- and/or nano-engineered platforms to fully realize useful devices for wide-scale application.

Acknowledgements

We thank Dr J. Howard for generously providing the kinesin expression clone. This work was supported by the Defense Advanced Research Projects Agency and Sandia's Laboratory Directed Research and Development Office. Sandia is a multi-program laboratory operated by Sandia Corporation, a Lockheed Martin Company, for the United States Department of Energy's National Nuclear Security Administration under Contract DE-AC04-94AL85000.

References

1 M. J. Feldstein, J. P. Golden, C. A. Rowe, B. D. MacCraith and F. S. Ligler, *Biomed. Microdevices*, 1999, **1**, 139–153.
2 R. Wiese, Y. Belosludtsev, T. Powdrill, P. Thompson and M. Hogan, *Clin. Chem.*, 2001, **47**, 1451–1457.
3 L. Rios and A. A. Garcia, *React. Funct. Polym.*, 2008, **68**, 307–314.
4 R. E. Biagini, D. L. Sammons, J. P. Smith, B. A. MacKenzie, C. A. F. Striley, V. Semenova, E. Steward-Clark, K. Stamey, A. E. Freeman, C. P. Quinn and J. E. Snawder, *Clin. Diagn. Lab. Immunol.*, 2004, **11**, 50–55.
5 J. T. Bookout, T. R. Joaquim, K. M. Magin, G. J. Rogan and R. P. Lirette, *J. Agric. Food Chem.*, 2000, **48**, 5868–5873.
6 K. Pettersson, H. Alfthan, U. H. Stenman, U. Turpeinen, M. Suonpaa, J. Soderholm, S. O. Larsen and B. Norgaardpedersen, *Clin. Chem.*, 1993, **39**, 2084–2089.
7 J. Leinonen, T. Lovgren, T. Vornanen and U. H. Stenman, *Clin. Chem.*, 1993, **39**, 2098–2103.
8 M. G. L. van den Heuvel and C. Dekker, *Science*, 2007, **317**, 333–336.
9 M. G. L. van den Heuvel, M. P. De Graaff and C. Dekker, *Science*, 2006, **312**, 910–914.
10 H. Hess, G. D. Bachand and V. Vogel, *Chem.–Eur. J.*, 2004, **10**, 2110–2116.
11 G. Steinberg, *Trends Microbiol.*, 2000, **8**, 162–168.
12 R. D. Vale, *Trends Biochem. Sci.*, 1999, **24**, M38–M42.
13 S. M. Block, *Trends in Cell Biology*, 1995, **5**, 169–175.
14 M. J. Schnitzer and S. M. Block, *Nature*, 1997, **388**, 386–390.
15 C. L. Asbury, A. N. Fehr and S. M. Block, *Science*, 2003, **302**, 2130–2134.
16 A. Yildiz, M. Tomishige, R. D. Vale and P. R. Selvin, *Science*, 2004, **303**, 676–678.
17 J. R. Dennis, J. Howard and V. Vogel, *Nanotechnology*, 1999, **10**, 232–236.
18 H. Hess, G. D. Bachand and V. Vogel, in *Dekker Encyclopedia of Nanoscience and Nanotechnology*, ed. J. Schwarz, C. Contescu and K. Putyera, American Scientific Publishers, New York, 2004, pp. 2201–2209.
19 A. Goel and V. Vogel, *Nature Nanotechnol.*, 2008, **3**, 465–475.
20 S. Taira, Y. Z. Du, Y. Hiratsuka, K. Konishi, T. Kubo, T. Q. P. Uyeda, N. Yumoto and M. Kodaka, *Biotechnol. Bioeng.*, 2006, **95**, 533–538.
21 C. M. Soto, B. D. Martin, K. E. Sapsford, A. S. Blum and B. R. Ratna, *Anal. Chem.*, 2008, **80**, 5433–5440.
22 M. Raab and W. O. Hancock, *Biotechnol. Bioeng.*, 2008, **99**, 764–773.
23 G. Bachand, S. Rivera, A. Carroll-Portillo, H. Hess and M. Bachand, *Small*, 2006, **2**, 381–385.
24 S. Ramachandran, K.-H. Ernst, G. Bachand, V. Vogel and H. Hess, *Small*, 2006, **2**, 330–334.
25 S. Taira, Y. Z. Du, Y. Hiratsuka, T. Q. P. Uyeda, N. Yumoto and M. Kodaka, *Biotechnol. Bioeng.*, 2008, **99**, 734–739.
26 C. Brunner, C. Wahnes and V. Vogel, *Lab Chip*, 2007, **7**, 1263–1271.

27 J. Clemmens, H. Hess, J. Howard and V. Vogel, *Langmuir*, 2003, **19**, 1738–1744.
28 J. Clemmens, H. Hess, R. Doot, C. M. Matzke, G. D. Bachand and V. Vogel, *Lab Chip*, 2004, **4**, 83–86.
29 H. Hess, J. Clemmens, C. Matzke, G. Bachand, B. Bunker and V. Vogel, *Appl. Phys. A*, 2002, **75**, 309–313.
30 H. Hess, C. M. Matzke, R. Doot, J. Clemmens, G. D. Bachand, B. C. Bunker and V. Vogel, *Nano Lett.*, 2003, **3**, 1651–1655.
31 J. R. Wasylycia, S. Sapelnikova, H. Jeong, J. Dragoljic, S. L. Marcus and D. J. Harrison, *Lab Chip*, 2008, **8**, 979–982.
32 R. Tucker, P. Katira and H. Hess, *Nano Lett.*, 2008, **8**, 221–226.
33 D. Wu, R. Tucker and H. Hess, *IEEE Trans. Adv. Pack.*, 2005, **28**, 594–599.
34 M. Uppalapati, Y. M. Huang, T. N. Jackson and W. O. Hancock, *Lab Chip*, 2008, **8**, 358–361.
35 S. Raviraja, Y. Wada, R. Sujatha, H. Hess and P. Satir, *Lab Chip*, 2006, **6**, 1239–1242.
36 M. Bachand, A. Trent, B. Bunker and G. Bachand, *J. Nanosci. Nanotechnol.*, 2005, **5**, 718–722.
37 G. D. Bachand, S. B. Rivera, A. K. Boal, J. Gaudioso, J. Liu and B. C. Bunker, *Nano Lett.*, 2004, **4**, 817–821.
38 D. L. W. Coy, M. and J. Howard, *J. Biol. Chem.*, 1999, **274**, 3667–3671.

